JACC VOL. 87, NO. 5, 2026

Myocardial Amyloid Burden in Transthyretin Amyloidosis

Awais Sheikh, MBChB,[a,*] Anouk Achten, MD,[b,*] Alberto Aimo, MD, PhD,[c,d] Yousuf Razvi, MBChB, BSc,[a] Josephine Mansell, MBBS, BMedSci,[a] Muhammad U. Rauf, MBBS,[a] Aldostefano Porcari, MD, PhD,[a,e,f] Rishi Patel, MBBS, PhD,[a] Lucia Venneri, MD, PhD,[a] Ana Martinez-Naharro, MD, PhD,[a] Carol Whelan, MD, PhD,[a] Cristina Quarta, MD, PhD,[g] Ruta Virsinskaite, MD,[a] Daniel Feffer Barak,[h] Ashutosh Wechalekar, MD,[a] Helen Lachmann, MD,[a] Daniel Knight, MBBS, MD (Res),[a,i] Tushar Kotecha, MD,[a] Peter Kellman, PhD,[j] Charlotte Manisty, MD, PhD,[k] James Moon, MD, MRCP,[k] Michele Emdin, MD, PhD,[c,d] Scott D. Solomon, MD,[l] Philip N. Hawkins, MBBS, PhD,[a] Julian Gillmore, MBBS, MD, PhD,[a,†] Marianna Fontana, MD, PhD[a,†]

ABSTRACT

BACKGROUND Stabilizers/silencers limit new transthyretin amyloid formation, whereas emerging agents aim to clear existing deposits. Cardiovascular magnetic resonance (CMR) extracellular volume (ECV) reflects myocardial amyloid and may provide a quantitative framework for therapeutic planning

OBJECTIVES The aim was to define calibrated ECV thresholds, evaluate their diagnostic and prognostic value, and explore how CMR-ECV could provide a quantitative framework for disease staging and therapeutic planning.

METHODS We studied 1,541 subjects undergoing CMR for transthyretin amyloidosis (ATTR) classified as *TTR*-variant carriers (n = 123), extracardiac ATTR (n = 41), early-stage ATTR-CM (n = 70), or overt ATTR-CM (n = 1,308). The endpoint was all-cause mortality.

RESULTS ECV was similar in carriers and extracardiac ATTR but rose from early-stage to ATTR-cardiomyopathy (CM). Associations with biomarkers, National Amyloidosis Centre (NAC) stage, Perugini grade, and echocardiographic measures were modest, with wide overlap. Diagnostic performance was excellent: ECV <30% excluded and ≥40% confirmed cardiac involvement, whereas 30% to 39% indicated early infiltration. Over a median follow-up of 2.8 years (IQR: 1.4-4.3 years), 612 patients (40%) died. Prognostically, ECV independently predicted mortality (HR: 1.22 per 10% increase; 95% CI: 1.10-1.34 per 10% increase; $P < 0.001$) after multivariable analysist. Stratifying patients by ECV categories (degree of infiltration: none <30%; mild = 30%-39%; moderate = 40%-49%; moderate-to-severe = 50%-59%; severe ≥60%) showed monotonic risk increase across categories. ECV retained prognostic value across hs-troponin and N-terminal pro-B-type natriuretic peptide (NT-proBNP) strata, Perugini grades 1 to 3, and left ventricular mass index (LVMI) tertiles, with steeper gradients in low-biomarker/low-LVMI strata.

CONCLUSIONS ECV directly quantifies myocardial amyloid load and, for the first time, defines reproducible thresholds that stratify burden and refine risk prediction beyond stage, biomarkers, and imaging, providing a quantitative framework for staging and therapeutic planning in ATTR amyloidosis. (JACC. 2026;87:505-518) © 2026 The Authors. Published by Elsevier on behalf of the American College of Cardiology Foundation. This is an open access article under the CC BY-NC-ND license (http://creativecommons.org/licenses/by-nc-nd/4.0/).

Listen to this manuscript's audio summary by Editor-in-Chief Dr Harlan M. Krumholz on www.jacc.org/journal/jacc/podcasts.

From the [a]National Amyloidosis Centre, University College London, Royal Free Campus, London, United Kingdom; [b]Department of Cardiology, Cardiovascular Research Institute Maastricht (CARIM), Maastricht University Medical Centre (MUMC+), Maastricht, the Netherlands; [c]Health Sciences Interdisciplinary Center, Scuola Superiore Sant'Anna, Pisa, Italy; [d]Cardiology Division, Fondazione Toscana Gabriele Monasterio, Pisa, Italy; [e]Center for Diagnosis and Treatment of Cardiomyopathies, Cardiovascular Department, Azienda Sanitaria Universitaria Giuliano-Isontina (ASUGI), University of Trieste, Trieste, Italy; [f]European Reference Network for Rare, Low Prevalence and Complex Diseases of the Heart-ERN GUARD-Heart, Trieste, Italy; [g]Alexion, AstraZeneca Rare Disease, Boston, Massachusetts, USA; [h]Humanitas University, Milan, Italy; [i]UCL Institute of Cardiovascular Science, University College London, Gower Street, London, United Kingdom; [j]National Heart, Lung, and Blood Institute, National Institutes of Health, Department of Health and Human Services, Bethesda, Maryland, USA; [k]Barts Heart Centre, London, United Kingdom; and the [l]Cardiovascular Division, Brigham and Women's Hospital, Harvard Medical School, Boston, Massachusetts, USA. *Drs Sheikh and Achten contributed equally to the work as first coauthors. †Drs Fontana and Gillmore contributed equally to the work as last coauthors.

ISSN 0735-1097 https://doi.org/10.1016/j.jacc.2025.10.054

ABBREVIATIONS AND ACRONYMS

ATTR = transthyretin amyloidosis

ATTR-CM = transthyretin amyloid cardiomyopathy

CMR = cardiovascular magnetic resonance

ECV = extracellular volume

hs-TNT = high-sensitivity troponin T

NT-proBNP = N-terminal pro-B-type natriuretic peptide

LVMI = left ventricular mass index

LVEF = left ventricular ejection fraction

NAC = National Amyloidosis Centre

Cardiac involvement in transthyretin (ATTR) amyloidosis spans a continuum: from genotype-positive carriers or very early disease with minimal/no cardiac signs, through subclinical or mildly symptomatic myocardial infiltration, to overt cardiomyopathy with heart failure. Severity varies across this spectrum and within transthyretin amyloid cardiomyopathy (ATTR-CM), in both variant ATTR (vATTR) and wild-type ATTR (wtATTR).[1,2]

Two therapeutic classes modify disease biology: TTR stabilizers reduce tetramer dissociation and significantly lower all-cause mortality and cardiovascular hospitalizations vs placebo,[3,4] whereas small-interfering RNA gene silencers suppress hepatic TTR production and also improve these outcomes.[5,6] Nonetheless, residual risk persists, with residual mortality remaining high, and quality of life and functional capacity continuing to decline in patients treated with these agents, supporting the need for approaches that clear existing amyloid deposits[7]; amyloid-depleting antibodies are now in clinical testing with signals of cardiac amyloid clearance.[8] Early data suggest that these agents may complement stabilizers and silencers by directly targeting and reducing the amyloid already deposited in the heart.[9] In this evolving landscape, the ability to directly quantify and stratify amyloid burden is becoming crucial, as this is the substrate future therapies aim to modify.

SEE PAGE 519

Cardiovascular magnetic resonance (CMR) is recommended for evaluating cardiac amyloidosis.[10,11] In cardiac amyloidosis, amyloid fibrils accumulate within the myocardial extracellular space, leading to expansion of the extracellular volume (ECV), which can be quantified noninvasively by CMR. Among CMR measures, ECV uniquely quantifies myocardial amyloid burden,[12] whereas biomarkers and echocardiography largely reflect downstream myocardial injury or functional consequences,[2] and thus ECV holds prognostic value in ATTR-CM: specifically, higher baseline ECV[13-15] and failure to stabilize ECV after initiation of treatment[15-17] predict mortality. However, previous studies have only reported crude associations between ECV and outcomes, which are not actionable. A consensus, threshold-based staging system using CMR-derived ECV has not been established, and validated prognostic staging remains biomarker based.[10,18] Defining calibrated, clinically meaningful ECV thresholds is essential to translate this measure from association to an implementable biomarker that can guide patient management and treatment strategies.[10,18]

The aim of this study was to calibrate and validate clinically meaningful ECV categories across the disease spectrum, assess their prognostic value, and position CMR-ECV as a framework for staging, risk prediction, and—potentially—future therapeutic planning.

METHODS

STUDY COHORT AND DIAGNOSTIC WORK-UP. Consecutive patients between 2011 and 2024 assessed at the National Amyloidosis Centre (NAC) in London were invited to participate in a prospective, protocolized clinical follow-up. Asymptomatic TTR variant carriers, patients with extracardiac TTR deposits, patients with early-stage ATTR-CM, and patients with overt ATTR-CM who underwent serial clinical assessment, routine biochemistry, echocardiography, and CMR imaging were included. Patients were classified participants into 4 prespecified categories.

- Asymptomatic *TTR* variant carriers: no myocardial uptake on technetium-99m-diphosphono-1,2-propanodicarboxylic acid (^{99m}Tc-DPD) scintigraphy; N-terminal pro-B-type natriuretic peptide (NT-proBNP) and troponin T within upper reference limits, and echocardiography judged normal for age by the evaluating cardiologists.
- Extracardiac ATTR: biopsy-proven peripheral ATTR deposits (eg, carpal tunnel tissue) with no clinical cardiac involvement as defined here.
- Early-stage ATTR-CM: Perugini grade 1 myocardial uptake on ^{99m}Tc-DPD scintigraphy, no monoclonal gammopathy, and biopsy-proven ATTR amyloidosis.
- Overt ATTR-CM: characteristic echocardiogram or CMR, and either direct endomyocardial biopsy proof of ATTR amyloid or presence of ATTR amyloid in an extracardiac biopsy along with cardiac uptake, or Grade 2 to 3 cardiac uptake in the

The authors attest they are in compliance with human studies committees and animal welfare regulations of the authors' institutions and Food and Drug Administration guidelines, including patient consent where appropriate. For more information, visit the Author Center.

Manuscript received September 22, 2025; revised manuscript received October 19, 2025, accepted October 21, 2025.

absence of biochemical evidence of a plasma cell dyscrasia.[19]

Patients were managed in accordance with the Declaration of Helsinki and provided written informed consent for analysis and publication of data (REC reference 21/PR/0620). Follow-up began with the date of CMR and was censored on December 2024. Mortality data were obtained via the UK Office of National Statistics.

CMR PROTOCOL. CMR imaging was conducted on a 1.5T clinical scanner (Magnetom Aera; Siemens Healthcare) using a standardized protocol. Cine images were obtained using a steady-state free precession (SSFP) sequence in both long-axis and short-axis orientations to assess biventricular volumes, mass, and systolic function. Native T1 mapping was performed with a Modified Look-Locker Inversion recovery (MOLLI) sequence in a 4-chamber long-axis view and at 3 short-axis levels. After intravenous administration of 0.1 mmol/kg of a gadolinium-based contrast agent (gadoterate meglumine [Dotarem, Guerbet S.A.]), postcontrast T1 mapping was repeated at 15 minutes at identical slice positions using the MOLLI sequence. Automated inline reconstruction of ECV maps was performed, with ECV values adjusted for hematocrit measured on the day of the scan. Late gadolinium enhancement (LGE) imaging was acquired using a phase-sensitive inversion recovery (PSIR) sequence, and the presence and distribution of LGE were assessed qualitatively. Image analysis was performed offline using Osirix MD 9.0. For ECV measurements, a single region of interest (ROI) was drawn in the basal to mid septum in the 4-chamber map. ECV values were categorized into 5 groups: <30%, no infiltration: 30% to 39%, mild infiltration; 40% to 49%, moderate infiltration; 50% to 59%, moderate-severe infiltration; ≥60%, severe infiltration. The 30% cutoff reflects reference values in healthy individuals,[20] whereas the other strata were prespecified in 10% ECV increments in the absence of established thresholds in the ATTR-CM setting.

STATISTICAL ANALYSIS. Analyses were performed in SPSS v24 (IBM), R (4.2.2) and Python (pandas, numpy, scikit-learn, matplotlib). Distributional assumptions were assessed with the Shapiro-Wilk test. Continuous variables are summarized as mean ± SD if normally distributed, otherwise as median (IQR); categorical variables as counts (percentages). Group comparisons across the 4 prespecified clinical categories (asymptomatic carriers, extracardiac ATTR, early-stage ATTR-CM, overt ATTR-CM) used nonparametric tests: Kruskal-Wallis for the overall comparison, followed by pairwise Wilcoxon rank-sum tests with Bonferroni correction for 6 comparisons (significance threshold $P < 0.008$). Categorical variables were compared using chi-square or Fisher exact tests, with pairwise P values reported in the tables and highlighted when significant after Bonferroni correction. For the comparisons between the prespecified ECV categories, P for trend was assessed using Jonckheere-Terpstra tests for continuous variables and the Cochran-Armitage trend test (or ordinal logistic regression) for proportions/ordinal variables. We also examined associations among ECV (dependent variable) and clinical, laboratory, and imaging covariates in

TABLE 1 Clinical, Laboratory, Echocardiography and Scintigraphy Findings

	Asymptomatic Carriers (n = 123)	Extracardiac ATTR (n = 41)	Early-stage ATTR-CM (n = 70)	Overt ATTR-CM (n = 1,308)
Age, y	55 (45-64)	81 (77-87)[a]	79 (70-88)[b]	80 (74-85)[c]
wt form	0 (0)	41 (100)[a]	48 (69)[b]	939 (72)
v genotype	123 (100)	0 (0)[a]	23 (33)[b]	369 (28)
Val122Ile	19 (15)	0 (0)[a]	2 (9)[b]	178 (14)
Other variants	104 (85)	0 (0)[a]	21 (91)[b]	190 (15)
Comorbidities				
Diabetes	8 (7)	4 (10)	7 (10)	182 (14)
Ischemic heart disease	1 (1)	9 (22)[a]	13 (19)[b]	237 (18)[c]
Hypertension	14 (11)	17 (42)[a]	17 (24)	433 (33)[c]
Atrial fibrillation	1 (1)	6 (15)[a]	14 (20)[b]	647 (50)[c,e,f]
NYHA functional class I/II/III/IV	120/3/0/0 (98/2/0/0)	32/9/0/0 (78/22/0/0)[a]	52/15/3 (74/21/4)[b]	1/202/904/201 (0/15/69/15)[c,e,f]
Laboratory exams				
NT-proBNP, ng/L	50 (50-87)	161 (95-305)[a]	247 (85-1009)[b]	2,528 (1,321-4,702)[c,e,f]
hs-troponin T, ng/L	4 (3-7)	12 (9-17)[a]	18 (11-28)[b,d]	58 (38-80)[c,e,f]
eGFR, mL/min/1.73 m^2	88 (76-90)	73 (58-84)[a]	72 (57-84)[b]	60 (48-75)[c,e,f]
NAC stage 1/2/3	119/2/0 (98/2/0)	38/2/0 (95/5/0)	59/8/3 (84/11/4)[b]	674/433/183 (52/34/14)[c,e,f]
Echocardiographic findings				
LV mean wall thickness, mm	10 (9-11)	11 (9-11)	12 (10-12)[b,d]	17 (15-18)[c,e,f]
E/e'	7 (6-10)	9 (7-11)	9 (7-11)[b]	15 (12-19)[c,e,f]
LVEF, %	60 (57-65)	60 (57-66)	59 (54-65)	50 (42-56)[c,e,f]
GLS, %	-19 (-21 to -17)	-19 (-22 to -17)	-18 (20 to -15)	-10 (-13 to -9)[c,e,f]
TAPSE, mm	23 (20-24)	25 (22-26)	20 (17-24)	15 (12-19)[c,e,f]
Perugini grade 0/1/2/3	123/0/0/0 (100/0/0/0)	35/4/0/0 (90/10/0/0)[a]	3/67/0/0 (4/96/0/0)[b,d]	1/18/1,054/224 (0/1/81/17)[c,e,f]

Values are median (IQR) or n (%). For categorical variables, the percentages were calculated out of the available values. Symbols indicate significant P values after the Bonferroni correction ($P < 0.008$) for the following comparisons: [a]Asymptomatic carriers vs extracardiac ATTR; [b]Asymptomatic carriers vs early-stage ATTR-CM; [c]Asymptomatic carriers vs overt ATTR-CM; [d]Extracardiac ATTR vs early-stage ATTR-CM; [e]Extracardiac ATTR-CM vs overt ATTR-CM; [f]Early-stage ATTR-CM vs overt ATTR-CM.

ATTR = amyloid transthyretin; CM = cardiomyopathy; eGFR = estimated glomerular filtration rate; GLS = global longitudinal strain; hs = high-sensitivity; LV = left ventricular; LVEF = left ventricular ejection fraction; NAC = National Amyloidosis Centre; NT-proBNP = N-terminal pro-B-type natriuretic peptide; TAPSE = tricuspid annular plane systolic excursion; v = variant; wt = wild type.

FIGURE 1 ECV Values Across the Spectrum of ATTR Disease

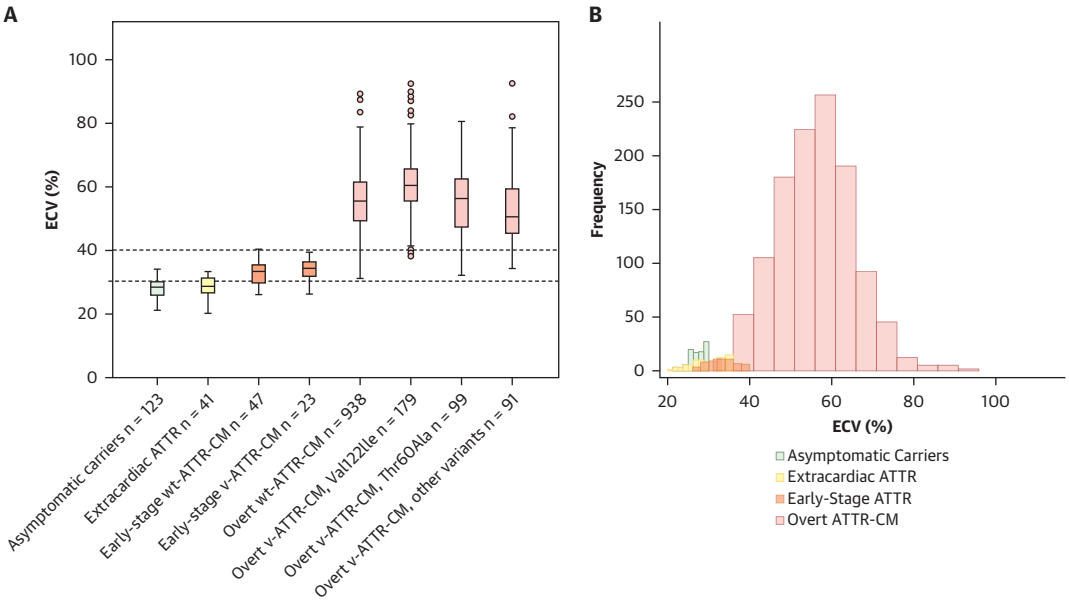

(A) Horizontal dashed lines mark the 30% and 40% ECV cutoffs. Subjects with wild-type (wt) vs variant (v) disease are reported separately. (B) Histogram of ECV distribution across the full cohort, stratified by disease category. Variant carriers, extracardiac ATTR, early-stage ATTR-CM, and overt ATTR-CM are shown in separate colors. ATTR-CM = transthyretin amyloid cardiomyopathy; ECV = extracellular volume.

separate univariable linear regressions. Before modeling, continuous covariates were ln-transformed (absolute global longitudinal strain [GLS] values used for ln-transformation); binary covariates were coded 1/0 and genotype wild type (wt) = 1, variant (v) = 2. We report standardized β coefficients with 2-sided *P* values and controlled family-wise error using Holm's method ($\alpha = 0.05$). Receiver operating characteristic (ROC) curves were generated for the following prespecified settings: 1) early or overt ATTR-CM in the whole cohort; 2) early ATTR-CM among individuals without overt ATTR-CM; 3) overt ATTR-CM in the whole cohort; and 4) overt ATTR-CM among individuals with any ATTR-CM (ie, either early or overt). We derived Youden J cutoffs, maximizing the combination of sensitivity and specificity and assessed the diagnostic performance of the 30% and 40% cutoffs in terms of sensitivity, specificity, positive, and negative prognostic value. We evaluated the incremental diagnostic value of cutoffs against 2 prespecified models: NT-proBNP + troponin + left ventricular mass index (LVMI)+ Perugini grade and NAC stage + troponin + LVMI + Perugini grade. Incremental value was quantified by likelihood-ratio tests for nested models, ΔAUC (DeLong's test), and category-free net reclassification improvement (NRI) and integrated discrimination improvement (IDI) with bootstrap 95% CIs. Diagnostic performance of ECV ≥30% and ECV ≥40% was also assessed across genotype and age tertiles. The endpoint was all-cause mortality; time zero was the CMR date, and patients were censored at study end. Kaplan-Meier curves compared survival across the 5 prespecified ECV strata with log-rank tests and numbers at risk displayed. Cox proportional-hazards models estimated HRs with 95% CIs for ECV, adjusted for age, sex, genotype (wt vs v), NAC stage, hs-troponin T, Perugini grade, LVMI, and left ventricular ejection fraction (LVEF). Unless otherwise specified, HRs for ECV refer to a 10% absolute increase (primary scale). For category-level presentation, risks were reported across the 5 ECV strata. Proportional-hazards assumptions were assessed using Schoenfeld residuals. To assess incremental prognostic performance of ECV on top of the multivariable model, we reported the change in Harrell's C-index (ΔC) and category-free NRI/IDI for 3-year risk using a landmark/time-dependent approach with bootstrap 95% CIs; model nesting was additionally compared by likelihood-ratio tests. Two-sided $\alpha = 0.05$ was used throughout; multiplicity was controlled with Bonferroni or Holm adjustments as specified here. Analyses used complete-case data.

TABLE 2 Findings Across ECV Categories

	ECV					
	<30% (n = 123)	**30%-39% (n = 148)**	**40%-49% (n = 260)**	**50%-59% (n = 484)**	**≥60% (n = 393)**	***P* for trend**
Age, y	59 (48-74)	75 (62-85)	82 (76-86)	81 (76-85)	78 (73-83)	**<0001**
wt form	37 (30)	77 (52)	189 (73)	372 (77)	264 (67)	**<0001**
NYHA functional class I/II/III/IV	109/9/0/0 (92/8/0/0)	100/39/4/0 (70/27/3/0)	61/171/27/0 (24/66/10/0)	67/346/70/0 (14/72/15/0)	42/271/80/0 (11/69/20/0)	**<0001**
NT-proBNP, ng/L	57 (50-118)	217 (84-625)	1,789 (803-3,298)	2,453 (1,296-4,536)	3,535 (2,148-5,780)	**<0001**
hs-troponin T, ng/L	7 (4-15)	17 (8-32)	41 (28-66)	59 (39-78)	69 (48-95)	**<0001**
eGFR, mL/min/1.73 m^2	86 (72-90)	75 (62-90)	63 (53-78)	61 (50-76)	57 (46-71)	**<0001**
NAC stage 1/2/3	109/6/1 (94/5/1)	132/8/2 (93/6/1)	169/64/23 (66/25/9)	257/161/59 (54/34/12)	153/162/72 (40/42/19)	**<0001**
Echocardiographic findings						
LV mean wall thickness, mm	10 (9-11)	11 (10-13)	15 (14-17)	17 (15-18)	18 (16-19)	**<0001**
E/e'	8 (6-10)	9 (7-13)	13 (11-16)	15 (12-19)	17 (13-21)	**<0001**
LVEF, %	60 (55-65)	60 (55-64)	54 (47-60)	51 (44-56)	45 (38-51)	**<0001**
GLS, %	-19 (-21 to -17)	-18 (-21 to -16)	-13 (-15 to -10)	-11 (-13 to -9)	-9 (-11 to -7)	**<0001**
TAPSE, mm	23 (18-24)	21 (17-25)	17 (14-20)	15 (13-20)	13 (11-16)	**<0001**
Perugini grade 0/1/2/3	102/14/0/0 (88/12/0/0)	50/46/41/5 (35/32/29/4)	1/8/229/21 (0/3/88/8)	0/7/403/68 (0/2/84/14)	0/1/279/109 (0/0/72/28)	**<0001**
CMR variables						
LV mean wall thickness, mm	10 (9-12)	12 (10-15)	17 (15-20)	19 (17-22)	21 (18-23)	**<0.001**
LVMI, g/m^2	60 (51-68)	69 (55-82)	102 (85-125)	122 (104-144)	138 (120-160)	**<0.001**
LVEDVi, mL/m^2	68 (59-77)	69 (59-80)	66 (57-78)	68 (58-80)	73 (60-85)	**<0.001**
LV SV index, mL/m^2	46 (40-51)	47 (40-53)	41 (35-47)	40 (33-50)	36 (31-43)	**<0.001**
LVEF, %	68 (63-72)	69 (63-74)	64 (51-71)	59 (50-67)	52 (43-60)	**<0.001**
MAPSE, mm	13 (11-14)	12 (10-13)	8 (6-10)	7 (6-9)	6 (5-8)	**<0.001**
Indexed LA area, cm^2/m^2	12 (10-13)	13 (12-15)	16 (14-19)	17 (15-19)	17 (15-19)	**<0.001**
RVEDVi, mL/m^2	75 (58-82)	75 (61-91)	69 (57-89)	69 (56-85)	73 (61-88)	**<0.001**
RVEF, %	64 (61-67)	64 (57-69)	58 (45-69)	55 (47-62)	48 (37-55)	**<0.001**
TAPSE, mm	22 (19-25)	20 (17-24)	14 (11-18)	12 (9-16)	10 (8-13)	**<0.001**
Native T1, ms	1,000 (976-1,025)	1,054 (1,028-1,084)	1,114 (1,083-1,138)	1,132 (1,103-1,160)	1,142 (1,111-1,176)	**<0.001**

Values are median (IQR) or n (%). Significant *P* values for trend are reported in **bold**.

ECV = extracellular volume; LA = left atrial; LVEDVi = left ventricular end-diastolic volume index; LVMI = left ventricular mass index; MAPSE = mitral annular plane systolic excursion; RVEDVi = right ventricular end-diastolic volume index; RVEF = right ventricular ejection fraction; SV = stroke volume; other abbreviations as in Table 1.

RESULTS

STUDY POPULATION AND SUBGROUPS. The study cohort included 1,541 subjects classified as asymptomatic carriers (n = 123, 8%), patients with extracardiac ATTR deposits (n = 41; 3%), early-stage ATTR-CM (n = 70; 5%), or overt ATTR-CM (n = 1,307; 85%). Two-thirds (n = 1,027; 67%) had no *TTR* gene variant, 200 (13%) carried Val122Ile, and 313 (20%) carried other *TTR* variants. The proportion of patients on disease-modifying use and trial participation at and after time of baseline CMR is summarized in Supplemental Table 1. Four patients were on tafamidis at baseline (median 4 months before CMR), whereas 388 initiated therapy during follow-up (median exposure 4 months) after tafamidis became routinely available in July 2024. Participation in other disease-modifying drugs and trials was also captured with median durations consistent with their respective study periods.

We compared clinical, laboratory, and echocardiographic variables across the 4 groups (asymptomatic carriers, extracardiac ATTR deposits, early-stage ATTR-CM, or overt ATTR-CM). Only hs-troponin T differed significantly across all pairwise comparisons, including asymptomatic carriers vs extracardiac ATTR. NT-proBNP and NYHA functional class also differed between these 2 groups, whereas NAC stage did not (**Table 1**).

In the whole cohort, ECV ranged from 20% to 92%, with a median of 53% (IQR: 44%-60%). ECV did not differ between asymptomatic carriers and

FIGURE 2 **ECV Categories Across Ranges of Cardiac Disease Metrics**

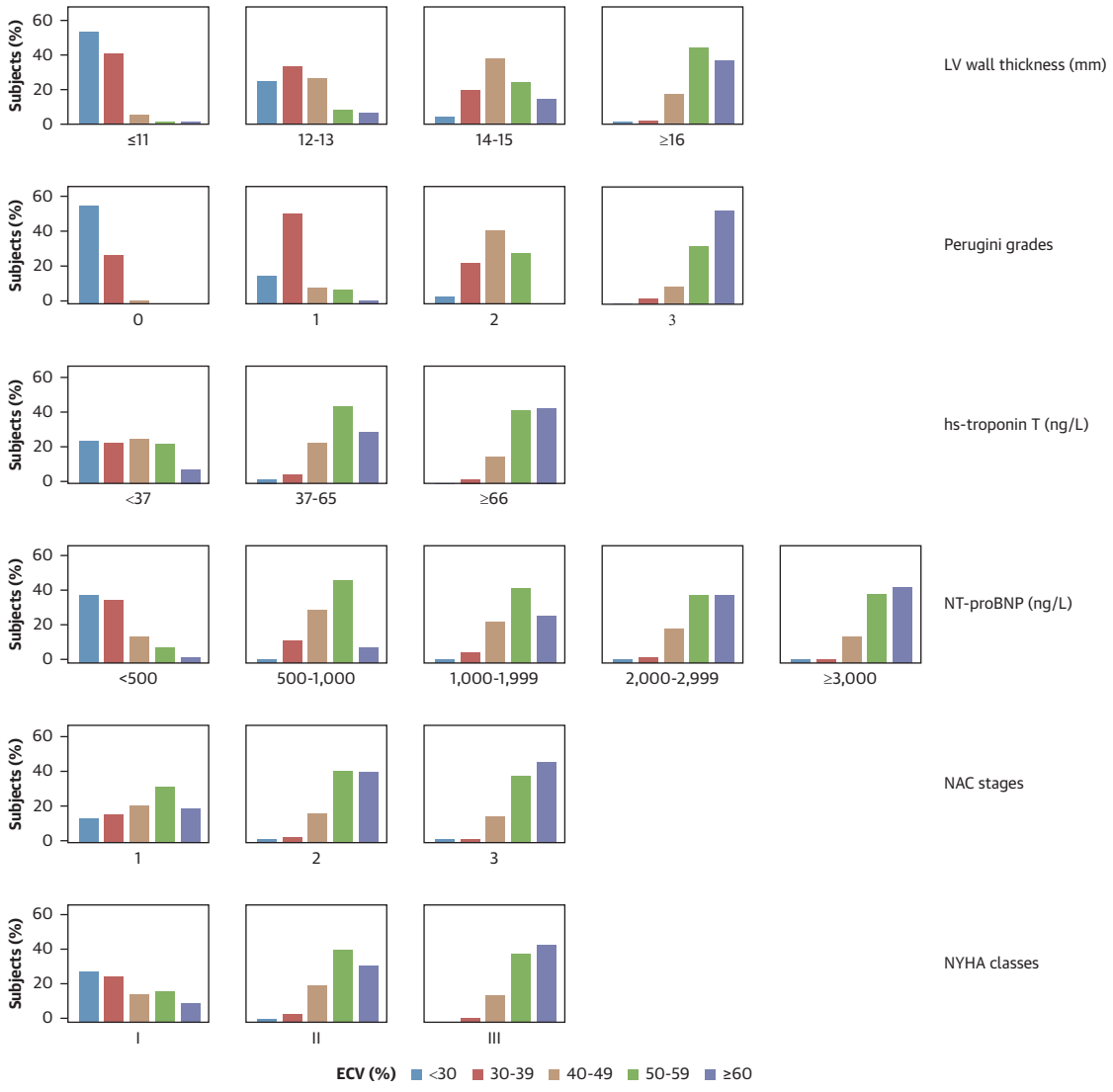

The percentages of subjects in the ECV ranges (<30%, 30%-39%, 40%-49%, 50%-59%, and ≥60%) in each subject category are reported. For continuous variables, tertiles are reported, except for N-terminal pro-B-type natriuretic peptide. hs = high-sensitivity; LVEF = left ventricular ejection fraction; NAC = National Amyloidosis Centre; other abbreviations as in Figure 1.

extracardiac ATTR (ie, those who did not display cardiac involvement), and started to increase only from early-stage ATTR-CM (Figure 1).

ECV VS INDICATORS OF CARDIAC INVOLVEMENT. ECV showed only modest-to-moderate associations across clinical, biomarker, scintigraphy, and echocardiographic measures, with consistently wide, bidirectional dispersion (Table 2, Figure 2, Supplemental Table 2). Cardiac biomarkers (hs-troponin T, NT-proBNP) rose on average with higher ECV, but values overlapped substantially, indicating that biomarkers are not interchangeable with tissue burden. ECV increased with NAC stage and Perugini grade on DPD scintigraphy, yet distributions overlapped (especially between grades 2 and 3), and stage 1 remained common even at higher ECV, so neither staging nor grading segregates amyloid load. Functional status tracked only loosely with substrate (many high-ECV patients were still NYHA functional class I to II). Echocardiographic structure (wall thickness, left ventricular [LV] mass) increased and deformation/right-sided indices (GLS, tricuspid

FIGURE 3 Association Between ECV and All-Cause Mortality Across Indicators of Cardiac Involvement: Forest Plot

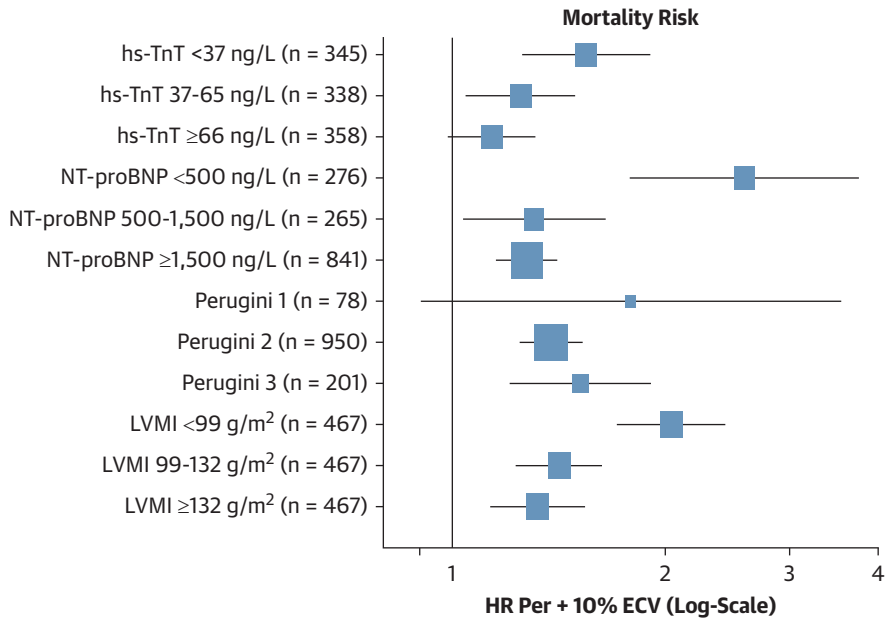

Within each subgroup, we ran a Cox model with ECV treated as a continuous variable. The HR shown is the change in risk of death per +10 percentage-points higher ECV (eg, from 35% to 45%). Square area is proportional to the number of patients in each subgroup. hs-TnT = high-sensitivity troponin T; LVMI = left ventricular mass index; NT-proBNP = N-terminal pro-B-type natriuretic peptide; other abbreviations as in Figure 1.

annular plane systolic excursion [TAPSE]) worsened with higher ECV, again with substantial within-stratum spread. Overall, dispersion was high and concordance low across modalities. We then considered different ranges of traditional metrics of cardiac involvement (cardiac biomarkers, Perugini grades, and LVMI). Across all stratifications, higher ECV was associated with higher mortality, and the association was most pronounced in patients with "low" classical indicators of cardiac involvement (lowest tertiles of hs-TnT and LVMI, and NT-proBNP <500 ng/L) (Figure 3).

ECV TO PREDICT CARDIAC INVOLVEMENT: DIAGNOSTIC CUTOFFS. We derived diagnostic cutoffs for either early or overt ATTR-CM in the whole cohort (n = 1,451), early ATTR-CM among individuals without overt disease (n = 234), and overt ATTR-CM either in the whole cohort (n = 1,451) or among individuals with early or overt ATTR-CM (n = 1,377) (Table 3).

TABLE 3 Diagnostic Performance of the 30% and 40% ECV Cutoffs

Condition Predicted	Group	Cutoff Method	ECV Threshold (%)	Sensitivity (%)	Specificity (%)	PPV (%)	NPV (%)
Early or overt ATTR-CM	Whole cohort	Youden	33	98	97	100	83
		ECV ≥30%	30	99	68	96	90
Early ATTR-CM	Nonovert ATTR-CM	Youden	31	74	79	58	88
		ECV ≥30%	30	81	68	50	90
Overt ATTR-CM	Whole cohort	Youden	39	98	98	100	89
		ECV ≥40%	40	96	99	100	84
Overt ATTR-CM	Early or overt ATTR-CM	Youden	40	96	98	100	58
		ECV ≥40%	40	96	98	100	58

NPV = negative predictive value; PPV = positive predictive value; other abbreviations as in Tables 1 and 2.

TABLE 4 Independent Prognostic Value of ECV and ECV Categories

	Model	HR (95% CI)	*P* Value
Absolute ECV values (per 10% increase)	Age, sex, wt/v disease, NAC stage, hs-troponin T, Perugini score, LVMI, LVEF	1.22 (1.10-1.34)	<0.001
ECV Categories			
<30%	Age, sex, wt/v disease, NAC stage, hs-troponin T, Perugini score, LVMI, LVEF	Reference	0.020
30%-39%		1.22 (1.10-1.34)	
40%-49%		1.49 (1.22-1.81)	
50%-59%		1.81 (1.35-2.43)	
≥60%		2.21 (1.49-3.26)	

Abbreviations as in Tables 1 and 2.

ECV discriminated extremely well between early/overt ATTR-CM and no cardiac involvement in the overall population (area under the curve [AUC] = 0.993). The Youden cutoff, representing the point that maximizes combined sensitivity and specificity, was 33% (Supplemental Table 3). The 30% ECV cutoff had 99% sensitivity and 68% specificity to exclude cardiac involvement.

In individuals without overt ATTR-CM (ie, asymptomatic carriers, patients with extracardiac ATTR deposits or with early-stage ATTR-CM), ECV had an AUC of 0.859 for identification of early-stage ATTR-CM. The Youden cutoff was 32%. The 30% ECV cutoff had 81% sensitivity and 68% specificity to exclude cardiac involvement.

FIGURE 4 Extracellular Volume Values and Survival: Spline-Curve Analysis

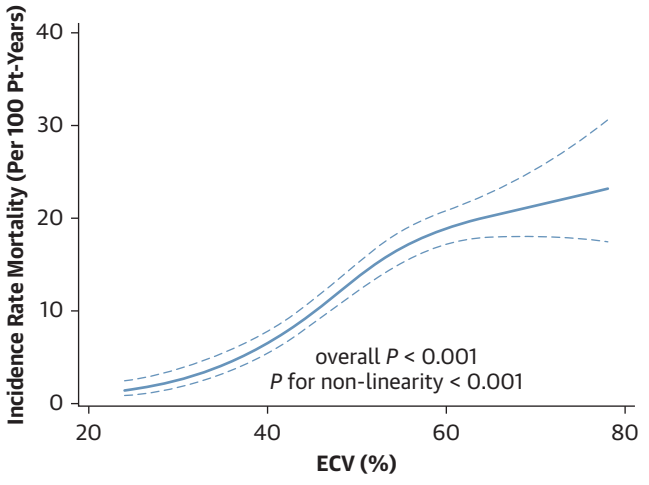

ECV = extracellular volume.

We then searched for cutoffs to predict overt ATTR-CM in the whole cohort. The Youden cutoff was 39%, and ECV 40% had 96% sensitivity and 99% specificity to predict overt ATTR-CM. Among individuals with either early or overt ATTR-CM, the Youden cutoff was 40%, and ECV 40% had 96% sensitivity and 98% specificity to predict overt ATTR-CM. The diagnostic performance of the 30% and 40% ECV cutoffs is reported in Table 2.

Findings were consistent across genotype (wt vs variant) and age tertiles, with ECV 30% and 40% cutoffs yielding comparable sensitivity and specificity in all subgroups (Supplemental Table 4).

We then evaluated the independent diagnostic value of cutoffs to multivariable models with NT-proBNP or NAC stage plus troponin, LVMI, and Perugini grade. Across all settings, the 30% and 40% ECV cutoffs added diagnostic information on top of biomarker-based models (Supplemental Table 5). Gains in AUC were small in which baselines were already near perfect, but reclassification improvements were consistent (Supplemental Table 6).

ECV 30% TO 39%: CHARACTERISTICS AND OUTCOME. We then focused on patients with ECV 30% to 39%, defining patients with early infiltration but no overt ATTR-CM. Age and sex distribution similar to the overall cohort, with variant genotype present in a minority. Biomarkers and imaging were often only modestly abnormal; median NT-proBNP and troponin were lower than in groups with ECV ≥40%, LVMI and LVEF were often in the normal range, and Perugini grade and NAC stages tended to be low to intermediate (Table 2).

ECV TO PREDICT CARDIAC INVOLVEMENT: RISK CATEGORIES. During a median follow-up of 2.8 years (IQR: 1.4-4.3 years), 612 patients (40%) died. In a multivariable prognostic model including age, sex, wt vs v genotype, NAC stage, hs-troponin T, Perugini grade, and CMR-derived LVMI and ejection fraction, absolute ECV values and ECV categories yielded independent prognostic value for mortality (Table 4).

When modeling risk according to ECV values, we observed a progressive increase in the 30% to 39% range and a further increase in risk for higher ECV values (Figure 4). Consistently, stratifying patients by ECV categories showed excellent survival for ECV <30% and a gradual decrease in survival for higher ECV categories (degree of infiltration: none <30%; mild = 30% to 39%; moderate = 40% to 49%; moderate to severe = 50% to 59%, severe ≥60%, infiltration) (Figure 5).

DISCUSSION

In this large, single-center cohort, CMR-derived ECV quantified myocardial amyloid burden across the full transthyretin amyloidosis spectrum, from genotype-positive carriers and patients with extracardiac deposits to early cardiac involvement and overt cardiomyopathy. Beyond simple association, this study moves further by providing calibrated, clinically meaningful categories that stratify infiltration into ranges, each carrying incremental prognostic value and potential relevance for future therapeutic planning. ECV rose stepwise across these groups, indicating that it captures substrate-level disease biology from the earliest detectable stages through advanced cardiomyopathy. In particular, ECV identified myocardial infiltration even when biomarkers and echocardiography low risk by conventional criteria (eg, normal echocardiography, NT-proBNP <500 ng/L, lowest troponin tertile, Perugini grade 1), supporting its role as an early disease marker capable of reclassifying patients before overt ATTR-CM is established. **Figure 6** summarizes how ECV complements indirect markers and refines risk stratification across predefined classes.

ECV was only modestly associated with conventional indicators of disease severity, including natriuretic peptides, high-sensitivity troponin T, NAC stage and NYHA functional class, Perugini grade, and echocardiographic measures. This discordance likely reflects that biomarkers and functional/structural indices primarily mirror downstream consequences of infiltration (myocyte stress, neurohormonal activation, remodeling), whereas ECV directly quantifies the extracellular amyloid substrate. This is particularly evident in early disease, in which ECV may rise before measurable wall stress, biomarker elevation, or structural change becomes apparent. Scintigraphy, although highly sensitive for detecting cardiac amyloid, does not provide a calibrated measure of burden. Taken together, the extent of myocardial amyloid cannot be reliably inferred from indirect measures alone, underscoring the nonexchangeability of these metrics with ECV (**Table 5**).

A key advance of this work is the definition of ECV categories with clear diagnostic and prognostic associations, which may inform future clinical frameworks and therapeutic planning (**Central Illustration**). From a diagnostic perspective, first, an ECV <30% reliably excluded cardiac involvement with high sensitivity, providing a practical rule-out/low risk anchor for clinical decisions. Second, an ECV ≥40% confirmed overt ATTR-CM with very high specificity. Importantly, diagnostic performance, and cutoff behavior were consistent across genotype and age bands, with only minor variations, reinforcing generalizability within the ATTR population. Between these anchors, the 30% to 39% band emerged as an intermediate zone in which ECV may be abnormal whereas biomarkers and other imaging appeared reassuring; outcomes were correspondingly intermediate, consistent with a stage of evolving infiltration. From a risk-stratification perspective, the amyloid burden as measured by ECV carried

FIGURE 5 ECV Categories and Survival: Kaplan-Meier Analysis

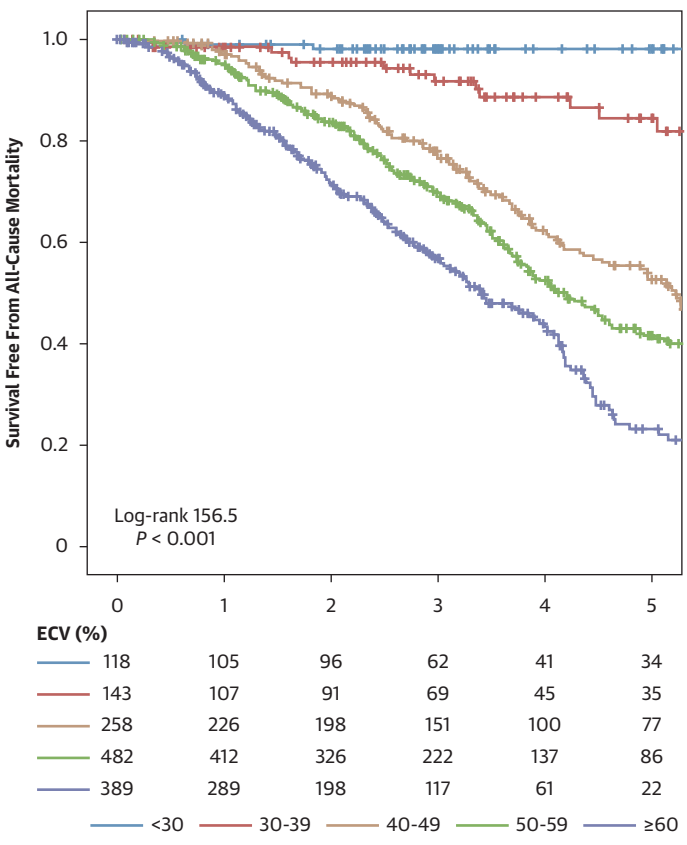

Kaplan-Meier curves showing survival free from all-cause mortality across predefined ECV categories (<30%, 30%-39%, 40%-49%, 50%-59%, and ≥60%). Increasing ECV was associated with a stepwise reduction in survival (log-rank chi-square = 156.5, $P < 0.001$). Numbers at risk are shown below the x-axis. Abbreviations as in **Figures 1 and 4**.

FIGURE 6 ECV Mapping Across the Spectrum of ATTR

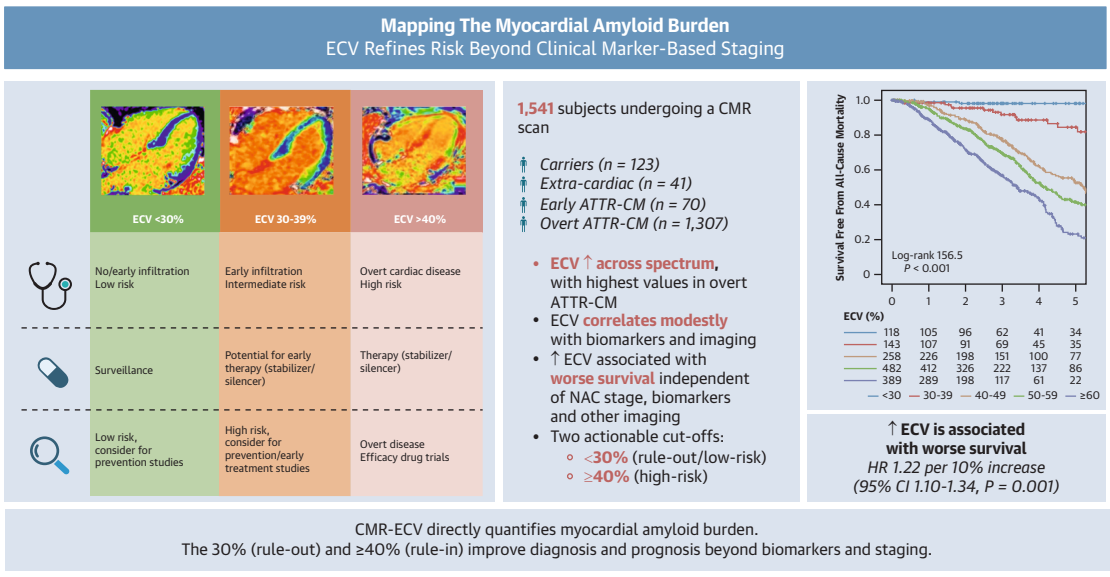

(Left) Representative 4-chamber CMR maps illustrate increasing myocardial ECV corresponding to low (<30%), intermediate (30%-39%), and high (>40%) amyloid burden. Each stage is accompanied by its clinical, therapeutic, and trial implications. (Center) Summary of the study population (n = 1,541) across the transthyretin amyloidosis spectrum, showing that ECV increases progressively from carriers and extracardiac to overt ATTR-CM. Higher ECV values correlate modestly with biomarkers and imaging indices and are independently associated with worse survival. (Right) Kaplan-Meier curves demonstrating survival stratified by ECV. An ECV <30% is associated with excellent prognosis, whereas ECV ≥40% identifies high-risk patients. Higher ECV was independently associated with worse survival (HR: 1.22 per 10% increase; 95% CI: 1.10-1.34; $P = 0.001$), after adjustment for age, sex, genotype, NAC stage, high-sensitivity Troponin, Perugini grade, and left ventricular ejection fraction. CMR = cardiac magnetic resonance; other abbreviations as in Figure 1.

independent prognostic information beyond established markers with survival declining in a graded fashion across predefined ECV strata (<30%, 30% to 39%, 40% to 49%, 50% to 59%, ≥60%). The prognostic effect of ECV was strongest in profiles in which biomarkers and echocardiography were least informative, reinforcing its early disease value. These findings align with the pathophysiology of ATTR-CM, in which outcomes reflect both ongoing fibril production and the burden of preexisting myocardial deposits. Notably, the distribution of ECV values was wide among patients with overt ATTR-CM but nearly always indicated at least moderate infiltration. Even individuals with only mild biomarker elevation or minimal symptoms exhibited substantial amyloid burden. This observation suggests that once ATTR-CM is diagnosed, myocardial infiltration is already significant, raising the hypothesis that amyloid-clearing therapies, once available, may need to be introduced earlier in the disease course—potentially in combination with stabilizers or silencers—rather than being reserved for advanced stages.

These results have practical implications. Stabilizers and silencers reduce new amyloid formation but residual risk persists; our data suggest that existing substrate burden independently influences prognosis. Quantitative assessment with CMR-ECV offers a substrate-level biomarker that can enhance patient selection and risk enrichment for future amyloid-clearing therapies and may serve as an objective framework for disease staging and longitudinal assessment in conjunction with established clinical and biomarker measures (Figure 7). An analogy is myocardial iron overload, in which therapy is guided by direct quantification (T2*); similarly, ECV may guide therapies that act on the amyloid substrate itself. In the context of trial readiness, our prespecified bands (<30%, 30% to 39%, 40% to 49%,

TABLE 5 Conceptual Table: Comparison of ECV With Other Metrics

Metric	Biological Target	Strengths	Limitations	Typical Range (Unit)	Prognostic Value	Actionability
CMR ECV	Amyloid burden	Direct, quantitative substrate-level measure; calibrated bands capture graded risk and define diagnostic threshold; complementary to biomarkers and echocardiography	Requires contrast and CMR access; thresholds require external validation	ECV <30%: Normal myocardium, no infiltration ECV 30%-39%: Early/ infiltration ECV ≥40% Overt ATTR-CM	Robust, independent, graded predictor of outcomes, directly linked to a key therapeutic target, informative in early disease and across the spectrum of ATTR-CM.	Substrate level measure of a key therapeutic target. Role in supporting trial design and risk enrichment; may inform future therapeutic planning and response monitoring as depleter strategies mature.
NT-proBNP	Myocyte wall stress/ neurohormonal activation	Widely available; standardized; part of staging systems; dynamic with congestion	Age/renal/AF/ fluid status dependent; reflects consequences, not amyloid burden; assay variability	Broad (hundreds–tens of thousands pg/mL); guideline "rule-in" thresholds are context-specific	Strong prognostic signal; integral to NAC staging when combined with troponin	Guides HF management and monitoring; not a direct amyloid burden measure
High-sensitivity troponin (eg, hs-cTnT)	Myocyte injury /necrosis	Widely available; reproducible; staging component	Assay-specific cutoffs; elevated in many comorbid states; not substrate specific	Normal typically <10-20 ng/L (assay-dependent); higher in ATTR-CM	Prognostic; contributes to NAC staging	Risk stratification and monitoring; not substrate quantification
Perugini grade (bone scintigraphy)	ATTR amyloid tracer uptake (semi-quantitative)	High diagnostic sensitivity/specificity for ATTR (with appropriate monoclonal protein testing); noninvasive	Semiquantitative; not calibrated for burden; reader/center variability; limited ability to track longitudinal changes	0 (none) to 3 (cardiac > bone)	Limited independent prognostic calibration vs ECV/biomarkers	Diagnostic classification; not a burden or dosing/response gauge. No ability to track treatment response.
LV mass (CMR/echo)	Combined measure of amyloid burden and myocyte	Ubiquitous; reproducible by CMR; tracks remodeling	Not specific to amyloid; geometry/sex/ BP dependent; may lag substrate change	Indexed LV mass: ~50–115 g/m^2 (men), ~43–95 g/m^2 (women); elevated in ATTR-CM varies	Modest incremental prognostic value versus biomarker/ ECV composites	Supports phenotyping and longitudinal remodeling assessment; indirect for amyloid burden

AF = atrial fibrillation; BP = blood pressure; CMR = cardiac magnetic resonance; HF = heart failure; other abbreviations as in Tables 1 and 2.

50% to 59%, ≥60%) demonstrate graded hazards and event rates that could enrich study populations: ≥40% identifies high-risk patients for efficacy trials, whereas 30% to 39% highlights earlier disease suitable for prevention studies.

STUDY LIMITATIONS. The principal limitation is that this is a single-center retrospective study from a national referral center, which may introduce selection bias and limit generalizability. The ECV cutpoints reported here are calibrated within this cohort; external, multicenter, and multivendor validation will be required to confirm these thresholds and their suitability for clinical decision making. ECV was acquired at 1.5 T using a standardized MOLLI protocol and a single basal-to-midseptal region of interest; future harmonization of acquisition and analysis across vendors will enhance comparability. Concomitant cardiac medications commonly used for management of heart failure were not systematically collected at the time of CMR and could not be incorporated in adjusted analyses; residual confounding from these therapies therefore cannot be excluded. The endpoint was all-cause mortality, and residual confounding from comorbidities or treatment heterogeneity cannot be excluded; prospective studies incorporating detailed therapeutic and longitudinal data are needed. Although systematic follow-up CMR was unavailable, previous work has

CENTRAL ILLUSTRATION **Myocardial Amyloid Burden in Transthyretin Amyloidosis**

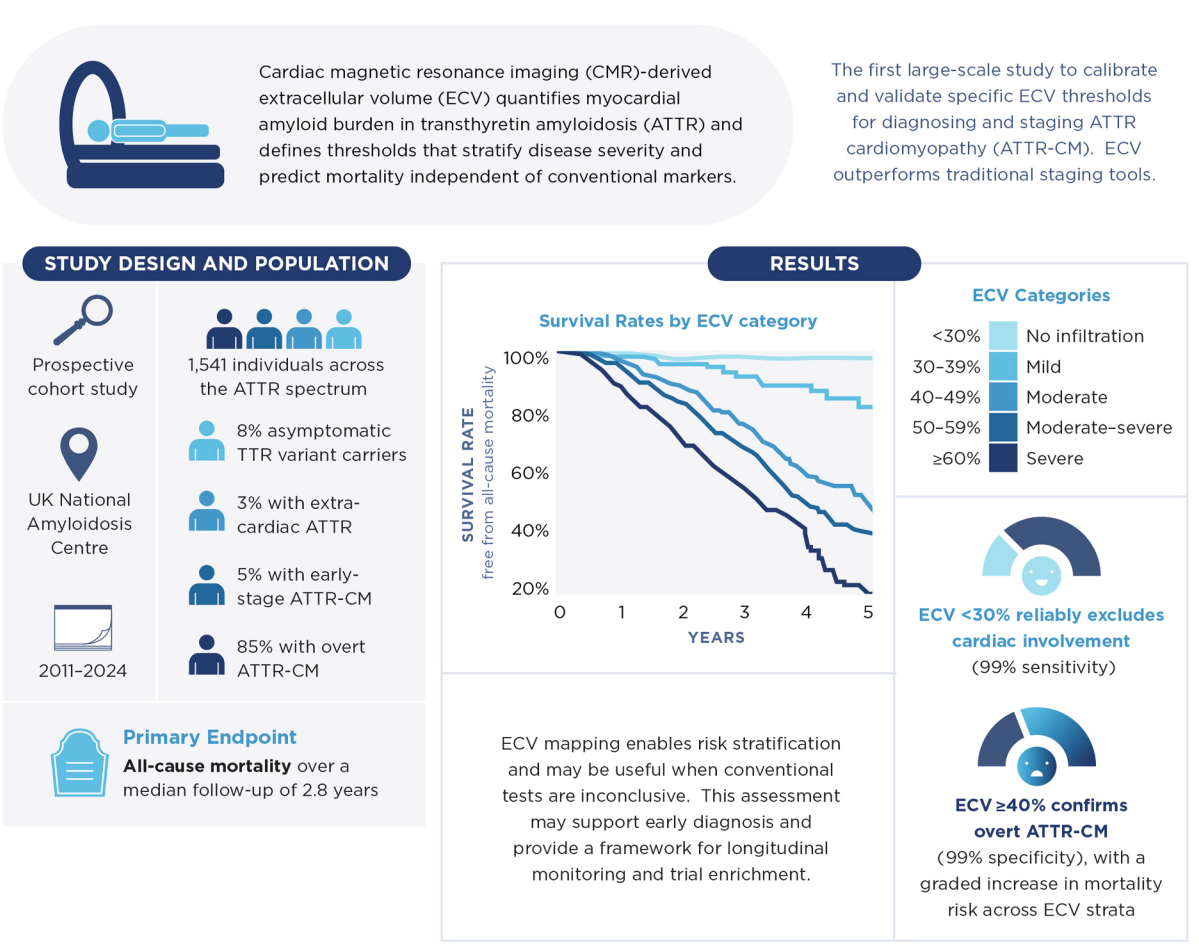

Sheikh A, et al. JACC. 2026;87(5):505–518.

shown that ΔECV predicts outcome, whereas this study defines absolute thresholds at which risk meaningfully increases, together establishing both dynamic (ΔECV) and absolute (threshold) dimensions of ECV as clinically relevant. Building on this framework, future work should test ECV-guided diagnostic and staging strategies against biomarker-based models, validate thresholds across centers, and evaluate ECV as a response biomarker in trials of amyloid-removing therapies. In earlier disease stages, ECV may identify individuals at highest risk of progression, and mechanistic correlations with histology and matrix remodeling could refine individualized treatment strategies.

CONCLUSIONS

As the field moves from discovery to intervention, the ability to calibrate amyloid burden with CMR-ECV transforms how we stage, monitor, and target ATTR-CM. These data establish ECV as a quantitative biomarker that bridges clinical practice and trial design, translating amyloid biology into actionable measurement. In the context of an expanding therapeutic landscape, which includes both agents targeting new amyloid production and therapies designed to clear existing deposits, ECV mapping may serve as a useful tool for disease staging, prognostication, and treatment planning in ATTR-CM.

FIGURE 7 **Conceptual Framework Linking ECV Thresholds to Disease Stage, Therapeutic Strategy and Research Applications in ATTR-CM**

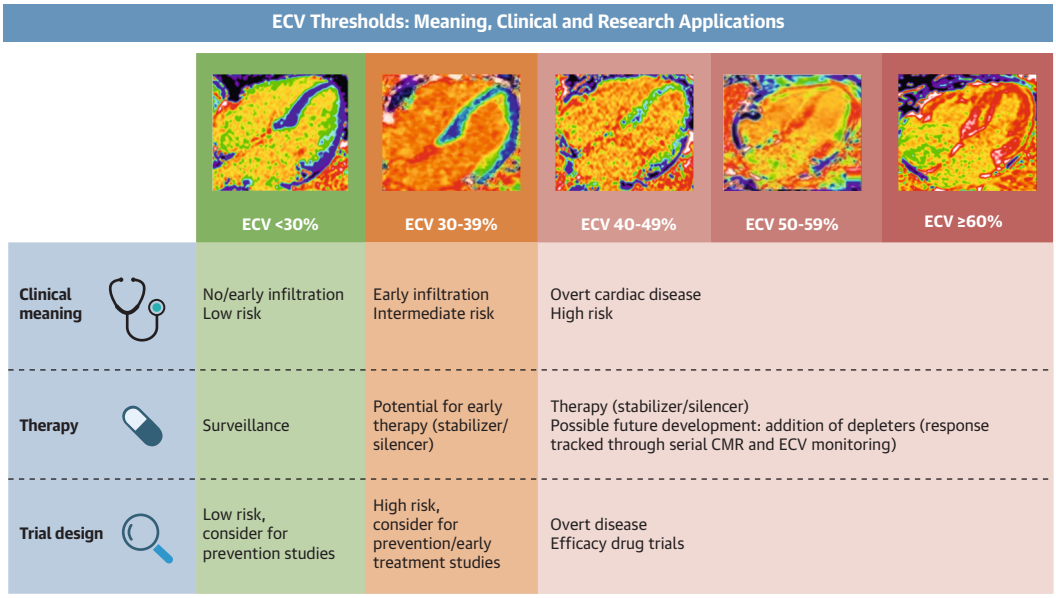

Representative 4-chamber ECV maps illustrate progressive myocardial amyloid infiltration across increasing ECV categories. The schematic relates ECV thresholds to corresponding clinical, therapeutic, and trial implications. Values <30% reflect normal myocardium with no infiltration; 30% to 39% represents early at-risk stages suitable for potential stabilizer or silencer therapy; ≥40% indicates established cardiac involvement that may warrant depleter therapy and serve as candidates for efficacy-endpoint clinical trials. Abbreviations as in Figure 1.

FUNDING SUPPORT AND AUTHOR DISCLOSURES

Dr Achten has received speakers honoraria from Pfizer paid to the Maastricht University Medical Centre; and has received consultancy honoraria from SAI MedPartners and Medcape. Dr Quarta is an employee of Alexion. Dr Manisty is a cofounder of Mycardium AI Ltd. Dr Moon is a shareholder of MyCardium AI Ltd. Dr Solomon has received research grants from Alexion, Alnylam, Applied Therapeutics, AstraZeneca, Bellerophon, Bayer, BMS, Boston Scientific, Cytokinetics, Edgewise, Bridgebio, Gossamer, GSK, Ionis, Intellia, Lilly, NIH/NHLBI, Novartis, NovoNordisk, Respicardia, Sanofi Pasteur, Tenaya, Theracos, and US2.AI; has consulted for Abbott, Action, Akros, Alexion, Alnylam, Amgen, Arena, Askbio, AstraZeneca, Bayer, BMS, Bridgebio, Cardior, Cardurion, Corvia, Cytokinetics, Intellia, GSK, Lilly, Novartis, Novo Nordisk, Roche, Theracos, Quantum Genomics, Tenaya, Sanofi-Pasteur, Dinaqor, Tremeau, CellProThera, Moderna, American Regent, Sarepta, Lexicon, Anacardio, Akros, Valo, Synhale, and Recordati; and has received research grants from Alexion, Alnylam, Applied Therapeutics, AstraZeneca, Bellerophon, Bayer, BMS, Boston Scientific, Cytokinetics, Edgewise, Bridgebio, Gossamer, GSK, Ionis, Intellia, Lilly, NIH/NHLBI, Novartis, Novo Nordisk, Respicardia, Sanofi Pasteur, Tenaya, Theracos, and US2.AI. Dr Gillmore has served as a consultant for Alnylam, ATTRalus, Ionis, Intellia, AstraZeneca, Bridgebio, Pfizer, and Lycia; and has received an institutional grant from Alnylam. Dr Fontana has received fees for consultancy for Alnylam, Alexion/Caelum Biosciences, Astrazeneca, Bridgbio/Eidos, Prothena, Attralus, Intellia Therapeutics, Ionis Pharmaceuticals, Cardior, Lexeo Therapeutics, Janssen Pharmaceuticals, Prothena, Pfizer, Novo Nordisk, Bayer, and Mycardium; has received research grants from Alnylam, Bridgbio, Astrazeneca, and Pfizer; has share options in LexeoTherapeutics; and has shares in Mycardium. All other authors have reported that they have no relationships relevant to the contents of this paper to disclose.

ADDRESS FOR CORRESPONDENCE: Dr Marianna Fontana, National Amyloidosis Centre, University College London, Royal Free Campus, Rowland Hill Street, London NW3 2PF, United Kingdom. E-mail: m.fontana@ucl.ac.uk.

REFERENCES

1. Lane T, Fontana M, Martinez-Naharro A, et al. Natural history, quality of life, and outcome in cardiac transthyretin amyloidosis. *Circulation*. 2019;140:16–26.

2. Fontana M, Ioannou A, Cuddy S, et al. The last decade in cardiac amyloidosis: advances in understanding pathophysiology, diagnosis and quantification, prognosis, treatment strategies, and monitoring response. *J Am Coll Cardiol Img*. 2025;18:478–499.

3. Maurer MS, Schwartz JH, Gundapaneni B, et al. Tafamidis treatment for patients with transthyretin amyloid cardiomyopathy. *N Engl J Med*. 2018;379:1007–1016.

4. Gillmore JD, Judge DP, Cappelli F, et al. Efficacy and safety of acoramidis in transthyretin amyloid cardiomyopathy. *N Engl J Med*. 2024;390:132–142.

5. Maurer MS, Kale P, Fontana M, et al. Patisiran treatment in patients with transthyretin cardiac amyloidosis. *N Engl J Med*. 2023;389:1553–1565.

6. Fontana M, Berk JL, Gillmore JD, et al. Vutrisiran in patients with transthyretin amyloidosis with cardiomyopathy. *N Engl J Med*. 2025;392:33–44.

7. Fontana M, Aimo A, Emdin M, et al. Transthyretin amyloid cardiomyopathy: from cause to novel treatments. *Eur Heart J*. https://doi.org/10.1093/eurheartj/ehaf667.

8. Garcia-Pavia P, Aus dem Siepen F, Donal E, et al. Phase 1 trial of antibody NI006 for depletion of cardiac transthyretin amyloid. *N Engl J Med*. 2023;389:239–250.

9. Fontana M, Gilbertson J, Verona G, et al. Antibody-associated reversal of ATTR amyloidosis-related cardiomyopathy. *N Engl J Med*. 2023;388:2199–2201.

10. Dorbala S, Ando Y, Bokhari S, et al. ASNC/AHA/ASE/EANM/HFSA/ISA/SCMR/SNMMI expert consensus recommendations for multimodality imaging in cardiac amyloidosis: Part 1 of 2: evidence base and standardized methods of imaging. *Circ Cardiovasc Imaging*. 2021;14:e000029.

11. Kittleson MM, Ruberg FL, Ambardekar AV, et al. 2023 ACC expert consensus decision pathway on comprehensive multidisciplinary care for the patient with cardiac amyloidosis: a report of the American College of Cardiology Solution Set Oversight Committee. *J Am Coll Cardiol*. 2023;81:1076–1126.

12. Scully PR, Bastarrika G, Moon JC, Treibel TA. Myocardial extracellular volume quantification by cardiovascular magnetic resonance and computed tomography. *Curr Cardiol Rep*. 2018;20:15.

13. Banypersad SM, Fontana M, Maestrini V, et al. T1 mapping and survival in systemic light-chain amyloidosis. *Eur Heart J*. 2015;36:244–251.

14. Martinez-Naharro A, Kotecha T, Norrington K, et al. Native T1 and extracellular volume in transthyretin amyloidosis. *J Am Coll Cardiol Img*. 2019;12:810–819.

15. Duca F, Rettl R, Kronberger C, et al. Myocardial structural and functional changes in cardiac amyloidosis: insights from a prospective observational patient registry. *Eur Heart J Cardiovasc Imaging*. 2023;25:95–104.

16. Patel RK, Ioannou A, Sheikh A, et al. Transthyretin amyloid cardiomyopathy: natural history and treatment response assessed by cardiovascular magnetic resonance. *Eur Heart J*. https://doi.org/10.1093/eurheartj/ehaf412.

17. Duca F, Poledniczek M, Kronberger C, et al. Serial extracellular volume quantification using cardiac magnetic resonance imaging in transthyretin amyloidosis patients treated with tafamidis. *Eur Radiol*. https://doi.org/10.1007/s00330-025-11792-x.

18. Garcia-Pavia P, Rapezzi C, Adler Y, et al. Diagnosis and treatment of cardiac amyloidosis: a position statement of the European Society of Cardiology Working Group on Myocardial and Pericardial Diseases. *Eur J Heart Fail*. 2021;23:512–526.

19. Gillmore JD, Maurer MS, Falk RH, et al. Nonbiopsy diagnosis of cardiac transthyretin amyloidosis. *Circulation*. 2016;133:2404–2412.

20. Sado DM, Flett AS, Banypersad SM, et al. Cardiovascular magnetic resonance measurement of myocardial extracellular volume in health and disease. *Heart*. 2012;98:1436–1441.

KEY WORDS cardiovascular magnetic resonance, extracellular volume, risk prediction, transthyretin amyloidosis

APPENDIX For supplemental tables and text, please see the online version of this paper.